Reac Kinet Mech Cat (2018) 123:313–322
https://doi.org/10.1007/s11144-017-1327-3

Synergistic SO_x/NO_x chemistry leading to enhanced SO_3 and NO_2 formation during pressurized oxy-combustion

Xuebin Wang[1,2] · Adewale Adeosun[1] · Grigory Yablonsky[1] · Akshay Gopan[1] · Pan Du[1] · Richard L. Axelbaum[1]

Received: 15 October 2017 / Accepted: 8 December 2017 / Published online: 16 December 2017

Abstract Pressurized oxy-combustion is a promising technology that can significantly reduce the energy penalty for CO_2 capture in coal-fired power plants. However, higher pressure might enhance the production of strong acid gases, including SO_3 and NO_2, which will lead to higher rates of corrosion. In this study, we investigated a reduced but combined SO_x and NO_x mechanisms and the synergistic formation of SO_3 and NO_2 was kinetically evaluated under different pressures and temperatures up to 15 atm and 1100 °C. The calculation results show that the interaction of SO_x and NO_x significantly accelerates the conversion rates of SO_2 to SO_3 and NO to NO_2, and the acceleration is much stronger at elevated pressures and comparatively low temperatures. With a strong interaction between SO_x and NO_x due to elevated pressures, the formation pathways of SO_3 and NO_2 through $HOSO_2 + O_2 = HO_2 + SO_3$ and $HO_2 + O = NO_2 + OH$, respectively, are dramatically promoted. These two reactions are linked by the reaction $SO_2 + OH + M = HOSO_2 + M$, resulting in a 'strong' cycle, which can be represented by the global reaction $NO + SO_2 + O_2 = NO_2 + SO_3$. This cycle is the major route for the formation and destruction of both SO_3 and NO_2 at elevated pressures.

Keywords Elevated pressure · SO_3 · NO_2 · Kinetic mechanism · Synergistic effect

✉ Richard L. Axelbaum
axelbaum@wustl.edu

[1] Consortium for Clean Coal Utilization, Energy, Department of Energy, Environmental & Chemical Engineering, Washington University in St. Louis, St. Louis, MO 63130, USA

[2] MOE Key Laboratory of Thermo-Fluid Science and Engineering, Xi'an Jiaotong University, Xi'an 710049, Shaanxi, China

Introduction

First-generation oxy-combustion technology, which operates under atmospheric pressure, suffers a significant penalty in net generating efficiency. By operating oxy-combustion under pressurized conditions, the plant efficiency can be increased because the latent heat in the flue gas moisture can be recovered and integrated into the steam cycle [1–3]. However, higher pressure enhances the production of strong acid gases, including NO_2 and especially SO_3, which could significantly increase the rate of corrosion. Thus, the formation of SO_3 during oxy-combustion has attracted attention in the past decade due to SO_x enrichment which is expected with flue gas recycle. A test conducted by Ahn et al. [4] in a pulverized coal (PC) furnace at the University of Utah found that the SO_3 produced in oxy-coal combustion is several times more than that in air combustion. A recent review of sulfur impacts in oxy-coal technology indicates that the quantity of SO_2 emission based on input coal mass (kg-SO_2/kg-coal) is reduced by 14–30%, depending on the coal type. Based on the sulfur mass balance, this suggests that the reduced sulfur mass must either be in the fly ash that are deposited on heating surfaces in the furnace or must have condensed as sulfuric acid [5]. These studies have demonstrated significant enhancement of SO_3 formation in oxy-combustion. However, previous studies were conducted at atmospheric pressures, and there are no reports on the formation of SO_3 under pressurized conditions, partially because at elevated pressure, accurate sampling and measurement of SO_3 is difficult. In addition, at elevated pressures, NO becomes easier to convert into NO_2, which particularly results in respiratory infections for adults and chronic lung injury for children [6].

Under POC conditions, the compression of the flue gas increases residence time in the furnace in proportion to the increase in operating pressure. Thus, the residence time in a POC furnace can be an order of magnitude or longer than that in atmospheric combustion. Thus, the formation of SO_3 through gas phase reactions could be significant with such a long residence time. In traditional atmospheric combustion processes, SO_3 is mainly catalytically formed in the selective catalytic reduction (SCR) De-NO_x unit and SO_3 formation in the gas phase can be neglected. At atmospheric pressure, SO_3 formation in the post-flame region is preferred via the oxidation of SO_2 [7–9]:

$$SO_2 + O + M = SO_3 + M \quad (R374)$$

and secondary formation via $HOSO_2$:

$$SO_2 + OH + M = HOSO_2 + M \quad (R376)$$

$$HOSO_2 + O_2 = SO_3 + HO_2 \quad (R422).$$

As seen above, SO_3 forms mainly through reactions in the O/H radical pool. Among the coexisting species in the post-flame region, NO_x has been proposed to influence SO_3 formation under certain conditions. The formation routes of NO_2 from NO are mostly via the following reactions, all of which affect the O/H radical pool:

$$NO + HO_2 = NO_2 + OH \quad (R186)$$

$$NO + O + M = NO_2 + M \quad (R187)$$

$$NO + O_2 = NO_2 + O \quad (R188).$$

On the basis of an analysis for atmospheric chemistry (1 atm), Song et al. [9] proposed a new process to oxidize NO and SO_2 in the flue gas simultaneously, and mentioned that reactions (R186, R376, and R422) can form a chain reaction to promote the formation of SO_3 and NO_2 if OH or HO_2 radicals are present. This hypothesis was verified in a recent measurement of SO_3 formation with NO addition in an atmospheric-pressure flow reactor [7]. Wei et al. [10] also observed the interaction between SO_x and NO_x when adding SO_2 into a coal flame in an entrained flow reactor (1 atm). Because all above studies have been performed at atmospheric pressure, the degree of this interaction was quite small. The only available measured data on SO_x and NO_x interaction at elevated pressures is presented by Mueller et al. [11] in a pressurized plug flow reactor at 950 K (0.5–10.0 atm) for a $CO/H_2O/O_2/NO/SO_2$ system. The pressurized results suggest that, at lower pressures, SO_3 formation occurs primarily through R1 and R3. However, the interaction via R424, given below, becomes important due to higher conversion ratio of NO to NO_2 at elevated pressures:

$$SO_2 + NO_2 = SO_3 + NO \quad (R424).$$

Integrated SO_x/NO_x removal technology is another motivation for studying SO_3 and NO_2 formation and interaction. This technology is considered a promising approach for flue gas purification and, potentially, for production of nitric and sulfuric acids in the gas processing unit of oxy-combustion systems [6, 12]. The concentrations of SO_x and NO_x at the inlet of the emission removal column have been shown to be critical to removal efficiency [13]. To date, the gas-phase interaction between SO_x and NO_x has been reported mainly for atmospheric pressure. However, at atmospheric pressure, conversion rates of NO to NO_2 and SO_2 to SO_3 in the post-flame region are very slow and residence times are short (e.g., 1–3 s). This is not the case at elevated pressures with a longer residence time. However, the formation of NO_2 and SO_3 in the gas phase and their interaction have not been adequately addressed for such pressurized systems.

This study seeks to understand the interaction mechanisms between SO_x and NO_x for evaluating the yield of strong acid gases, specifically SO_3 and NO_2, in the post-flame region of the POC process. After validating the detailed mechanism (72 species and 428 reactions) including nitrogen and sulfur chemistry based on its comparison with the literature experimental data, the synergistic promotion of SO_3 and NO_2 was kinetically evaluated under representative post-flame conditions, and the effects of temperature and pressure on this synergistic promotion were studied. The rate of production was used to illustrate SO_x/NO_x interaction mechanism, and to demonstrate the formation routes of SO_3 and NO_2.

Methods

This study adopts a detailed gas-phase mechanism including nitrogen and sulfur chemistry based on GRI-Mech 3.0 [14]. The mechanism includes 72 species and 428 steps, in which the subset of sulfur and SO_x/NO_x interactions are from Glarborg et al. [15] and Mueller et al. [11], respectively. CHEMKIN software package is employed assuming plug flow [8]. The conditions studied are chosen so as to represent the post-flame conditions of POC (1–15 atm, 700–1100 °C). Before using the detailed mechanism to predict SO_3 and NO_2 formation under POC conditions, nine cases are compared with experimental results from literatures [11, 16, 17]. The comparison indicates that the mechanism can accurately predict the evolution of SO_3 and NO_2 in the complex environment under both atmospheric and elevated pressures. In this study, rate-of-production (ROP) analysis is employed because it is a useful tool in understanding reacting-flow calculations, which determines the contribution of each reaction to the net production or destruction rates of certain species [18]. In addition, ROP analysis allows for quick identification of dominant reaction paths.

Results and discussion

The synergistic promotion of SO_3 and NO_2 formation at varied pressures and temperatures

To identify the synergistic effect between SO_x and NO_x at various pressures (1–15 atm) and temperatures (700–1100 °C), the formation of SO_3 with and without the coexistence of NO are compared in Fig. 1. Likewise, the formation of NO_2 with and without the coexistence of SO_2, are compared in Fig. 2 under the same pressures and temperatures. The major gas composition is selected as $O_2 = 5\%$, $H_2O = 15\%$, with CO_2 as the balance gas. In Fig. 1, the inlet SO_2 concentration is 1000 ppm and NO concentration is shifted between 0 and 1000 ppm, while in Fig. 2, the inlet NO concentration is 1000 ppm and SO_2 concentration is shifted between 0 and 1000 ppm. In Fig. 1, we observe a synergy between SO_3 and NO_2 formation for all conditions, with the degree of promotion significantly dependent on operating pressure and temperature. At elevated pressure and lower temperature,

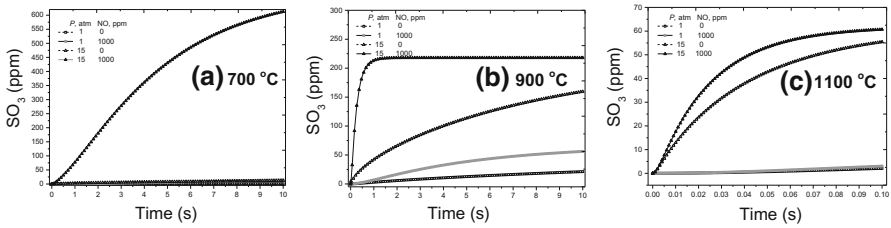

Fig. 1 SO_3 formation with and without SO_x–NO_x coexisting (SO_2 = ppm, $O_2 = 5\%$, $H_2O = 15\%$, CO_2 as the balance of the gas; for the dashed line, NO = 1000 ppm; for the solid line, NO = 0 ppm)

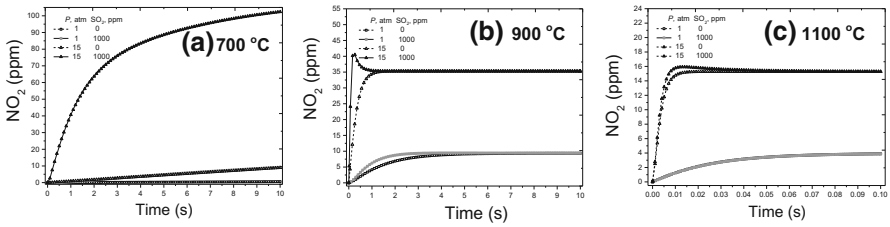

Fig. 2 NO_2 formation with and without SO_x–NO_x coexisting (NO = 1000 ppm, O_2 = 5%, H_2O = %, CO_2 as the balance of the gas; for the dashed line, SO_2 = 1000 ppm; for the solid line, SO_2 = 0 ppm)

SO_3 and NO_2 formations are promoted. However, at higher temperatures above 1100 °C and atmospheric pressure, the effect of this interaction is negligible. In an atmospheric-pressure coal-fired furnace, the residence time in the post-flame region is about 2 s. As shown in Fig. 1, at 1 atm and a time scale of 2 s, the maximum SO_3 formation occurs at 900 °C, and the conversion ratio from SO_2 to SO_3 is only 1.65% (SO_3, 16.5 ppm) and 0.60% (SO_3, 6 ppm) with and without NO addition, respectively. In contrast, under POC conditions (e.g., 15 atm), the residence time in the post-flame region can be longer than 10 s. As shown in Fig. 1, in the temperature range from 700 to 1100 °C and at 15 atm, the conversion ratio from SO_2 to SO_3 can vary from about 5% (SO_3, 50 ppm) to 60% (SO_3, 600 ppm), depending on temperature. Such a high SO_3 formation ratio indicates that low-temperature corrosion in the furnace and in the wet FGR unit of pressurized oxy-combustion system could be severe, and it will be necessary to implement specific measures to address SO_3 before the flue gas temperature approaches acid dew point. For example, in the POC process designed by Washington University in St. Louis, a direct contact cooler (DCC) is used to remove SO_x/NO_x- simultaneously before the flue gas temperature drops below the acid dew point [1, 19].

On the other hand, the synergistic effect also accelerates the formation of NO_2, as observed from Fig. 2. This acceleration is comparatively weak at temperatures above 900 °C at which the NO_2 formation reaches equilibrium within 10 s. The conversion ratio from NO to NO_2 is as low as 1.5–3.5% (NO_2, 15–35 ppm) under POC conditions (15 atm). At a lower temperature of 700 °C, the conversion ratio from NO to NO_2 increases to above 10% under POC conditions (15 atm). Moreover, we observe that NO_2 reaches equilibrium before SO_3, for all conditions studied. These observations are discussed further in "Reaction pathway analysis on the formation of SO_3 and NO_2 at elevated pressure (15 atm)" section.

Reaction pathway analysis on the formation of SO_3 and NO_2 at elevated pressure (15 atm)

These results presented above show that the SO_x–NO_x interaction promotes significantly the formation of SO_3 and NO_2 within a certain temperature range and at elevated pressure. In this section, to better illustrate the effect of SO_x–NO_x interaction on SO_3 and NO_2 formation under these specific conditions, we analyze the formation pathway of SO_3 and NO_2 formation at elevated pressures with and

without SO_x–NO_x interaction. Based on this analysis and sensitivity studies, a 9-step reduced chemistry is developed.

SO_3 and NO_2 formation pathway without SO_x–NO_x interaction at elevated pressure (15 atm)

SO_3 formation To better illustrate the effect of SO_x–NO_x interaction on SO_3 and NO_2 formation at elevated pressures, we perform reaction pathway analyses on SO_3 and NO_2 formation without SO_x–NO_x interaction, and the results of the ROP analysis are shown in Figs. 3 and 4 for SO_3 and NO_2, respectively.

In Fig. 3 at elevated pressure of 15 atm, SO_3 is formed dominantly through the oxidation of $HOSO_2$ by O_2 (R422) regardless of temperature. At 1100 °C, the preferred formation route is via the oxidation of SO_2 by O radical, which is typically neglected in atmospheric conditions i.e., R374.

$$SO_2 + O(+\ M) = SO_3(+M) \quad (R374).$$

In addition, R381, which is the oxidizing reaction by HO_2, becomes an important route at lower temperature regions, e.g., at 700 °C,

$$SO_2 + HO_2 = SO_3 + OH \quad (R381).$$

NO_2 formation As shown in Fig. 4, at elevated pressure (15 atm), the formation of NO_2 is mainly via the oxidation by HO_2 (R186), O (R187), and O_2 (R188) independent of temperature, which are the same as the reaction routes at atmospheric pressure mentioned earlier. We also note that the contribution of each reaction varies significantly with temperatures. In this study, the route via R186 by HO_2 oxidation is dominating at the higher temperature, 1100 °C and R187 and R188 by O and O_2 oxidation are dominant at the lower temperatures. As shown in Fig. 4, none of these three routes (R186, R187, and R188) can be neglected at a medium temperature, say for example 900 °C.

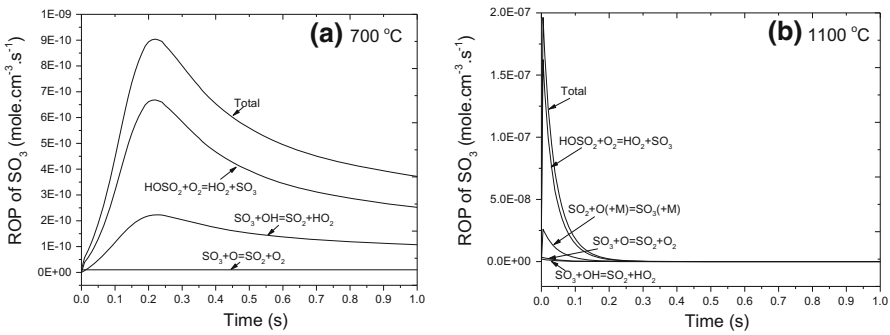

Fig. 3 ROP analyses on SO_3 formation without SO_x–NO_x interaction (15 atm, SO_2 = 1000 ppm, O_2 = 5%, H_2O = 15%, CO_2 as the balance of the gas)

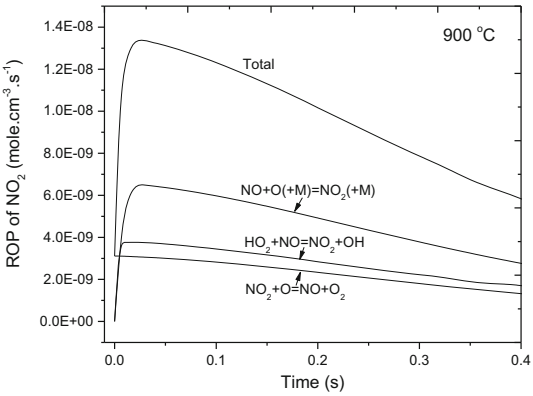

Fig. 4 ROP analyses on NO_2 formation without SO_x–NO_x interaction (15 atm, NO = 1000 ppm, O_2 = 5%, H_2O = 15%, CO_2 as the balance of the gas)

SO_3 and NO_2 formation pathway with SO_x–NO_x interaction at elevated pressure (15 atm)

Under conditions where SO_x and NO_x coexist at elevated pressure (15 atm), ROP analysis results for SO_3 and NO_2 formation are shown in Fig. 5. Compared with the ROP analysis results in Figs. 3 and 4, when SO_x and NO_x do not coexist, a significant contribution to SO_3 formation and NO_2 destruction from reaction R424 is noticeable, and this agrees with the experimental results of Mueller et al. [11]. The net reaction rate of molecular reaction R424 is determined by the concentrations of SO_2, NO_2, SO_3 and NO_2, and is important for the SO_x–NO_x system to reach equilibrium.

$$SO_2 + NO_2 = SO_3 + NO \quad (R424).$$

Under the conditions evaluated and before the system reached equilibrium, R424 retains the forward direction, producing SO_3 but consuming NO_2. This explains the phenomenon observed in Fig. 2 where NO_2 reaches equilibrium much earlier than SO_3 in the environment with coexisting SO_x–NO_x. Routes for NO_2 formation (Figs. 5b) also exhibit a big difference if SO_x and NO_x coexist in the reactive

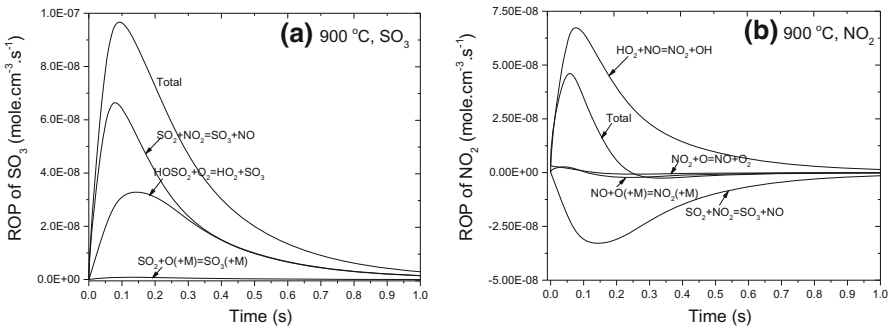

Fig. 5 ROP analyses on (**a**) SO_3 and (**b**) NO_2 formation with SO_x–NO_x interaction (15 atm, SO_2 = 1000 ppm, NO = 1000 ppm, O_2 = 5%, H_2O = 15%, CO_2 as the balance of the gas)

Table 1 The dominant reaction pathway of SO_3 and NO_2 formation at elevated pressures (unit: mol, s, K, cal)

New number	Old number	Reaction	*A*	β	*E*	Source
SR1	R87, R287	$OH + HO_2 = O_2 + H_2O$	2.89×10^{13}	0	− 497	Baulch et al. [20]
SR2	R186	$HO_2 + NO = NO_2 + OH$	2.11×10^{12}	0	− 480	GRI-Mech 3.0 [14]
SR3	R376	$SO_2 + OH(+M) = HOSO_2(+M)$	5.70×10^{12}	− 0.3	0	Li et al. [21]
SR4	R422	$HOSO_2 + O_2 = HO_2 + SO_3$	7.80×10^{11}	0	656	Li et al. [21]
SR5	R424	$SO_2 + NO_2 = SO_3 + NO$	6.30×10^{12}	0	27,000	Armitage and Cullis [22]

mixture. With SO_x–NO_x coexisting at 15 atm, the only notable route for NO_2 formation is via R186 by HO_2 oxidation, while the routes via R187 and R188 by O and O_2 oxidation become unimportant. At high temperatures of 900 and 1100 °C, because of the rapid production of NO_2 at the initial stage, the backward reaction pathway of R187 is favored, leading to the consumption of NO_2, another reason for the NO_2 reaching equilibrium earlier than SO_3 especially at higher temperatures.

The dominant reaction pathway of SO_3 and NO_2 formation at elevated pressures

Based on the above analysis, a dominant reaction pathway of SO_3 and NO_2 formation at elevated pressures can be obtained, which mainly includes five reaction steps (R87/287, R186, R376, R422, R424). These five reaction steps rearranged and renamed in Table 1 with SR# denoting the reaction number (e.g., 'SR1' means the first reaction in this reaction pathway). These five reactions of skeletal mechanism can be classified into three groups: (1) SR1 is the initiation reaction step that triggers production of initial OH and HO_2 radicals which allows cyclic reactions to occur; (2) SR2-SR4 are the cyclic reaction group and they are important pathways for producing SO_3 and NO_2, and (3) SR5 is an important pathway for more production of SO_3 but the consumption of NO_2.

Conclusions

In the present work, the synergy between SO_x and NO_x mechanisms was investigated and its role on the formation of SO_3 and NO_2 was kinetically evaluated under different pressures and temperatures, using a developed detailed mechanism based on GRI-Mech 3.0. The main conclusions are as follows:

The interaction of SO_x and NO_x significantly accelerates the conversion rates of SO_2 to SO_3 and NO to NO_2, and the acceleration is much stronger at elevated pressures and lower temperatures. Due to the strong interaction between SO_x and NO_x, the formation pathways of SO_3, through $HOSO_2 + O_2 = HO_2 + SO_3$, and NO, through $HO_2 + NO = NO_2 + OH$, are dramatically promoted. These two pathways are linked by the reaction $SO_2 + OH + M = HOSO_2 + M$, resulting in a 'strong' cycle, which can be represented by the global reaction $NO + SO_2 + O_2 = NO_2 + SO_3$. This cycle together with $SO_2 + NO_2 = SO_3 + NO$ dominate the formation and destruction of both SO_3 and NO_2 at elevated pressures.

Acknowledgements The authors gratefully acknowledge the financial support of the National Key Research and Development Program of China (No. 2016YFB0600605), the National Natural Science Foundation of China (Nos. 51676157 and 5161101654), the U.S. Dept. of Energy (Award # DE-FE0009702), and the Consortium for Clean Coal Utilization (CCCU) at Washington University in St. Louis. We would also like to thank Mr. James Ballard at Washington University in St. Louis for editing the manuscript for language errors.

References

1. Axelbaum RL, Kumfer B, Wang X (2016) Advances in pressurized oxy-combustion for carbon capture. CornerStone 4(2):52–56
2. Hong J, Chaudhry G, Brisson JG, Field R, Gazzino M, Ghoniem AF (2009) Analysis of oxy-fuel combustion power cycle utilizing a pressurized coal combustor. Energy 34(9):1332–1340
3. Gopan A, Kumfer BM, Axelbaum RL (2015) Effect of operating pressure and fuel moisture on net plant efficiency of a staged, pressurized oxy-combustion power plant. Int J Greenh Gas Control 39:390–396
4. Ahn J, Okerlund R, Fry A, Eddings EG (2011) Sulfur trioxide formation during oxy-coal combustion. Int J Greenh Gas Control 5:S127–S135
5. Stanger R, Wall T (2011) Sulphur impacts during pulverised coal combustion in oxy-fuel technology for carbon capture and storage. Prog Energy Combust Sci 37(1):69–88
6. Santos S, Duarte A, Bordado J, Gomes J (2016) New process for simultaneous removal of CO_2, SO_x and NO_x. Ciência & Tecnologia dos Materiais 28(2):106–111
7. Lutz AE, Kee RJ, Miller JA (1988) SENKIN: A FORTRAN program for predicting homogeneous gas phase chemical kinetics with sensitivity analysis. Sandia National Labs, Livermore
8. Larson RS (1996) PLUG: A Fortran program for the analysis of plug flow reactors with gas-phase and surface chemistry. Sandia Labs, Livermore
9. Design R (2010) CHEMKIN/CHEMKIN-PRO theory manual CHEMKIN® Software. August, pp 1–360
10. Wei X, Han X, Schnell U, Maier J, Wörner H, Hein KR (2003) The effect of HCl and SO_2 on NO_x formation in coal flames. Energy Fuels 17(5):1392–1398
11. Mueller M, Yetter R, Dryer F (2000) Kinetic modeling of the $CO/H_2O/O_2/NO/SO_2$ system: implications for high-pressure fall-off in the $SO_2 + O\ (+M) = SO_3\ (+M)$ reaction. Int J Chem Kinet 32(6):317–339
12. Gomes J, Santos S, Bordado J (2015) Choosing amine-based absorbents for CO_2 capture. Environ Technol 36(1):19–25
13. Ting T, Stanger R, Wall T (2013) Laboratory investigation of high pressure NO oxidation to NO_2 and capture with liquid and gaseous water under oxy-fuel CO_2 compression conditions. Int J Greenh Gas Control 18:15–22
14. Smith GP, Golden DM, Frenklach M, Moriarty NW, Eiteneer B, Goldenberg M, Bowman CT, Hanson RK, Song S, Gardiner Jr, W (2011) GRI-Mech 3.0, 1999. URL http://www.me.berkeley.edu/gri_mech
15. Glarborg P, Kubel D, Dam-Johansen K, Chiang HM, Bozzelli JW (1996) Impact of SO_2 and NO on CO oxidation under post-flame conditions. Int J Chem Kinet 28(10):773–790
16. Dayma G, Dagaut P (2006) Effects of air contamination on the combustion of hydrogen—effect of NO and NO_2 addition on hydrogen ignition and oxidation kinetics. Combust Sci Technol 178(10–11):1999–2024
17. Wang X, Li S, Adeosun A, Li Y, Vujanović M, Tan H, Duić N (2017) Effect of potassium-doping and oxygen concentration on soot oxidation in O_2/CO_2 atmosphere: a kinetics study by thermogravimetric analysis. Energy Convers Manag 149:686–697
18. Design R (2007) CHEMKIN theory manual. San Diego
19. Gopan A, Kumfer BM, Phillips J, Thimsen D, Smith R, Axelbaum RL (2014) Process design and performance analysis of a staged, pressurized oxy-combustion (SPOC) power plant for carbon capture. Appl Energy 125:179–188
20. Baulch D, Cobos C, Cox R, Frank P, Hayman G, Just T, Kerr J, Murrells T, Pilling M, Troe J (1994) Evaluated kinetic data for combustion modeling. Supplement I. J Phys Chem Ref Data 23(6):847–848
21. Li B, Sun Z, Li Z, Aldén M, Jakobsen JG, Hansen S, Glarborg P (2013) Post-flame gas-phase sulfation of potassium chloride. Combust Flame 160(5):959–969
22. Armitage J, Cullis C (1971) Studies of the reaction between nitrogen dioxide and sulfur dioxide. Combust Flame 16(2):125–130